Preliminary morphological and biochemical changes in rat liver following postnatal exposure to sodium arsenite

Arnab Bhattacharya, Pushpa Dhar, Raj D. Mehra

Department of Anatomy, All India Institute of Medical Sciences, New Delhi, India

Abstract: The effects of sodium arsenite exposure on the hepatic maturation period of cellular and functional reorganization in developing rat livers were evaluated. Animals received intraperitoneal injections of sodium arsenite (1.5 mg/kg body weight) or distilled water on days 9 to 28 after birth. On day 29, the animals were sacrificed either by cervical dislocation or by perfusion fixation. The perfusion fixed liver tissue was processed for paraffin embedding, sectioning and hematoxylin and eosin staining. The fresh liver tissue was processed for cryo-sectioning followed by Sudan Black B staining and for biochemical estimation of reduced glutathione. Microscopic observation revealed comparable preserved hepatic lobular patterns and distributions of uninucleate and binucleate hepatocytes in the control and the experimental groups. The mean nuclear area and diameter of the hepatocytes was increased in the experimental group. Lipid droplet distribution pattern in Sudan Black B stained sections revealed higher staining intensity towards the centrilobular area in both groups. Semiquantitative estimation of staining intensity showed lower mean gray values in zone 3 than in zones 2 and 1 (suggestive of the setting in of the adult pattern) in both groups. The reduced glutathione levels in the liver tissue and the altered nuclear size of the hepatocytes in the experimental group suggested the impairment of morphological and biochemical processes induced by arsenic exposure during the postnatal period.

Key words: Arsenic, Wistar rats, Liver, Morphometry, Sudan Black B, Reduced glutathione

Received March 22, 2012; Revised September 15, 2012; Accepted October 25, 2012

Introduction

Arsenic is an environmental pollutant of global concern. Inorganic arsenic in polluted drinking water is the chief source of exposure to arsenic in the Ganga-Meghna-Brahmaputra basin of India and Bangladesh [1]. Acute exposure to high concentrations of arsenic is highly toxic and fatal [2]; however, the effects of sustained exposure to lower concentrations are less clearly defined. Arsenic exposure can lead to toxic effects in the nervous, the cardiovascular, the respiratory, the integumentary and the hepatobiliary systems [3]. In the hepatobiliary system, the liver remains the center of metabolic activity during the fetal period and after birth [4]. The profound changes in the environment of the developing liver after birth, in the form of its blood supply, its adaptation to the diurnal rhythm of eating etc., determine cell reorganization and the development of various cyclic processes [5]. In rats, this period of great cellular and functional reorganization corresponds to postnatal days (PND) 9-28; maturation is completed by PND 28 [5]. In humans, it corresponds to the fifth postnatal year [5]. The developing liver is highly vulnerable to endogenous and

Corresponding author:
Pushpa Dhar
Department of Anatomy, All India Institute of Medical Sciences, Room No. 1036, Teaching Block, First Floor, New Delhi 110029, India
Tel: +91-011-26593225, Fax: +91-011-26588641, E-mail: dharpushpa@hotmail.com

exogenous insults during this period. The infantile exposure to arsenic has been reported to lead to morbidity in adult life [6-9]. This work reports the effects of postnatal exposure to sodium arsenite on rat livers. Maturation parameters are studied: the conversion of double cell plates to single cell plates [5]; the increase in size of hepatocytes and their nuclei [10] and the centrilobular distribution of lipid droplets [11].

Materials and Methods

Animals

Pregnant female Wistar rats were from the Experimental Animal Facility of the All India Institute of Medical Sciences. The study was approved by the Institute Ethics Committee.

Experimental diet

The animals were provided with a standard rodent diet and drinking water *ad libitum*. They were maintained on 12-hour light/dark cycles under controlled temperature and humidity.

Experimental design

The day of birth of the pups was considered postnatal day zero (PND 0). The mother-reared pups were divided into a control group (I) and an experimental group (II) (n=12/group). They received intraperitoneal injections of double distilled, pyrogen-free, sterile water (group I) or aqueous sodium arsenite (1.5 mg/kg body weight, group II) from PND 9 to 28. The animals were sacrificed on PND 29. During the experimental period, the animals were weighed daily and various developmental signs were noted (eye opening,

development of fur, etc.). Each group was further divided into subgroups "a & b" (n=6). The experimental design is summarized in Fig. 1.

The animals of groups Ia and IIa (Fig. 1) were sacrificed under ether anaesthesia followed by trans-cardiac perfusion with 4% paraformaldehyde in 0.1 M phosphate buffer. The liver was dissected out and tissue from the right and the left lateral lobes was further processed for paraffin embedding. Serial sections (7 μm) were cut and stained with hematoxylin and eosin (H&E).

The animals of groups Ib and IIb (Fig. 1) were sacrificed by cervical dislocation under ether anaesthesia and processed for cryosectioning and Sudan Black B (SBB) staining.

Sampling

The pups were randomly assigned to the control or experimental group, each containing 12 pups. These groups were further randomly divided into subgroups, each with 6 pups, for the obtaining of fresh and paraformaldehyde fixed liver tissue post sacrifice.

Biochemical assay

The middle lobe of the liver (fresh unfixed; groups Ib and IIb) was weighed, sliced and homogenized at a final concentration of 20% in water [12]. To 0.5 ml of this homogenate, 20% trichloroacetic acid and 0.6 mM ethylene diaminetetraacetic acid were added to a final volume of 1 ml. This solution was centrifuged (2,000 rev./min for 5 minutes). To 0.2 ml supernatant, was added 2 ml 0.6 mM Ellman's reagent (5,5'-dithiobis-2-nitrobenzoic acid; DTNB) in 0.2
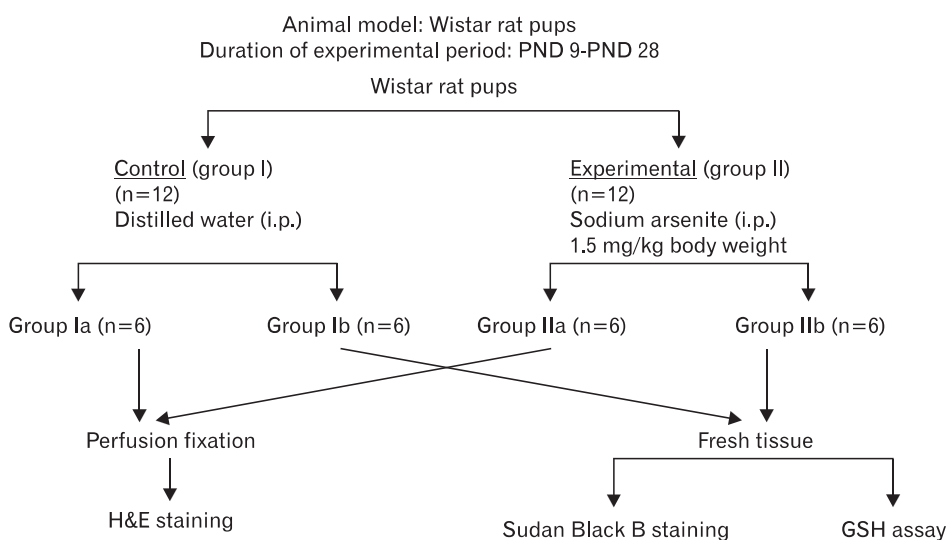

Fig. 1. Experimental design. GSH, glutathione; i.p., intra-peritoneal; PND, post natal days.

M phosphate buffer (pH 8.0) to a final volume of 3 ml. This was pipetted into a well of an enzyme linked immunosorbent assay plate. Each reaction was carried out in duplicates and the absorption was read at 415 nm against a reagent blank [12] to assay tissue's reduced glutathione content [13].

Histology and histochemistry

H&E and SBB staining procedures were employed.

Animals in groups Ia and IIa (Fig. 1) were anaesthetized with ether before trans-cardiac perfusion with 4% paraformaldehyde in 0.1 M phosphate buffer. The liver was dissected out and tissue pieces from the right and the left lateral lobes were further processed for paraffin embedding. Serial sections (7 μm) were cut and stained with H&E.

Animals in groups Ib and IIb (Fig. 1) were sacrificed by cervical dislocation under ether anaesthesia. Fresh liver tissue from the right and the left lateral lobes were immersion fixed in cold 4% paraformaldehyde in 0.1 M phosphate buffer and further processed for cryosectioning and SBB staining. Briefly, 20 μm thick cryocut sections were dehydrated in ascending grades of ethanol up to 70% and stained with a saturated solution of SBB in 70% ethanol (90 minutes). After washing in 70% ethanol, the slides were immersed in tap water before mounting with glycerine [14-16].

Photomicrography

Sections were observed using a Nikon Eclipse E600 microscope and photographed using a digital camera (DS-Fi1, Nikon, Melville, NY, USA).

Morphometric assessments

The H&E and SBB stained sections were separately morphometrically analyzed. Taxonomy, the counting of uni- and bi-nucleate cells, and nuclear area, and equivalent nuclear diameter, were assessed in groups Ia and IIa. Optical density (OD), a marker of the density of lipid accumulation, was measured in groups Ib and IIb.

For morphometric analysis of H&E stained sections, digital photomicrographs were captured to measure the area and the equivalent diameter of hepatocytes' nuclei under 40× (pixel size, 0.24 μm/pixel). One randomly chosen section of each sample, incorporating both right and left lateral lobes, and ten randomly chosen fields/sections were considered for measurement, so that a minimum of fifty hepatocytes per sample were measured [17]. Heptatocytes with a prominent nucleolus within the nucleus were considered for

measurement [18]. A standard rectangular grid (270×80 μm^2) was placed on the section and the uninucleate and binucleate hepatocytes within the measured grid area were counted (Fig. 2A). Cells contacting the left and the lower margins of the grid were not counted.

The SBB stained sections were observed by optical microscopy with image analysis software (NIS-Elements AR 3.1, Nikon). The chosen fields were converted to gray scale of 0 (black)-255 (white). In each field, three rectangular grids of equal area were placed between the central vein and the portal triads in question (half area of a classical liver acinus). The grid areas were numbered 3, 2, 1 from the central vein towards the portal triad (Fig. 2B) [19]. The mean intensity of staining was proportional to the amount of lipid localized in each grid zone. Twenty five such fields were observed for each
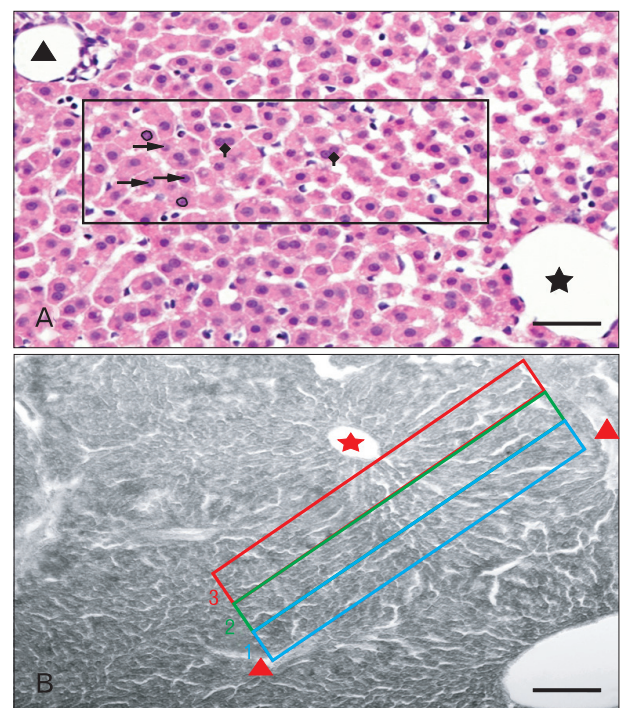

Fig. 2. High magnification photo micrographs of (A) hematoxylin and eosin stained and (B) Sudan Black B stained sections of liver (postnatal days [PND] 29). (A) A standard rectangular grid (270 μm× 80 μm) between the central vein (black asterisk) and the portal triad (black triangle). The nuclear area and equivalent diameter of the nuclei were generated by encircling the nuclear outline after selecting tool AREA (circle). Uninucleate (➡), binucleate (➡) cells (NIS Elements AR 3.1 software). (B) Three rectangular grids of equal area between the central vein (red asterisk) and the inter portal triad region (red triangle) dividing the parenchyma centrifugally into zones (3, 2, 1), from which the mean gray value of each grid area and mean gray value per zone were measured. Scale bars=20 μm (A), 50 μm (B).

lobe (left and right lateral) per sample [20] and the gray values were pooled to obtain a mean gray value. For each group, the mean gray value from six animals was taken as the final gray value for the group.

Statistical analysis

The morphometric parameters' mean±SD were computed for each lobe (right and left lateral) of each liver. The values were compared between the control and the experimental groups using Mann Whitney U and Kruskalwallis tests. The mean reduced glutathione levels of the individual samples of each group were treated as clustered data, and their differences were compared between the groups by Mann Whitney U testing. The OD data were subjected to Mann Whitney U testing and Kruskalwallis testing to evaluate the difference in staining intensity on zonal basis, if any, between the control and the experimental animals. SPSS ver. 17 (SPSS Inc., Chicago, IL, USA) was used for the analysis and $P<0.05$ were considered significant in all the tests.

Reagents and stains

All reagents and stains were from Sigma Aldrich (St. Louis, MO, USA).

Results

General features

Various developmental features (ear unfolding, development of fur and spontaneous quadruped walking with the ventral surface of body off the floor) appeared at the scheduled times in both groups of animals. There was no observed difference in the two goups' general activities such as food intake, alertness and movement.

Body weight

The groups' growth, measured daily by body weight, showed progressive and comparable increases in body weight from PND 1 to 9, before arsenic was first introduced to group II (Fig. 3A). On PND 29 (the day of sacrifice), the body weight of groups I and II, 54.8±13.79 g and 51.8±11.52 g, respectively, had tripled from the values at PND 9 (Fig. 3B). The control group showed a marginally higher weight gain.

No apparent gross abnormality in the liver's shape or lobar pattern was observed in either group.

Microscopic observations (H&E stained sections)

The lobular pattern, with the central vein in the center and the portal triads in the periphery, was clearly evident in both groups (Fig. 4A, B). The radially arranged plates of hepatocytes (with a single nucleus) between the adjacent sinusoids (Fig. 4C) were regular in outline and directed from the central vein of each lobule towards its periphery. The sinusoids, lined by flat endothelial cells and Kupffer cells, appeared somewhat larger in group II (Fig. 4D). The hepatocytes, larger in group II, appeared as large polyhedral cells with acidophilic cytoplasm. The central spherical nucleus, with a sharply outlined nuclear membrane, exhibited large prominent nucleoli and peripherally dispersed chromatin. Binucleate cells were also distributed throughout (Fig. 4E, F). Vacuoles (Fig. 5B) were observed in the hepatocytes near the
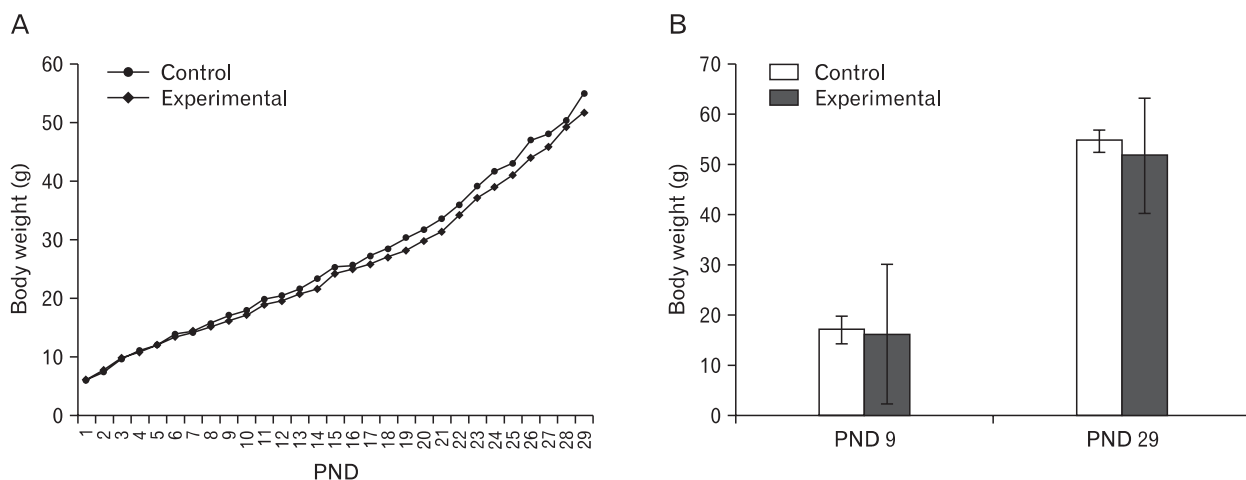

Fig. 3. Linear growth curve based on daily recorded weight (postnatal days [PND] 1 to 29) (A); bar diagram showing body weight at PND 9 (beginning of the treatment period) and PND 29 (day of sacrifice) (B) of the control and the experimental groups. Values expressed as mean±SD.
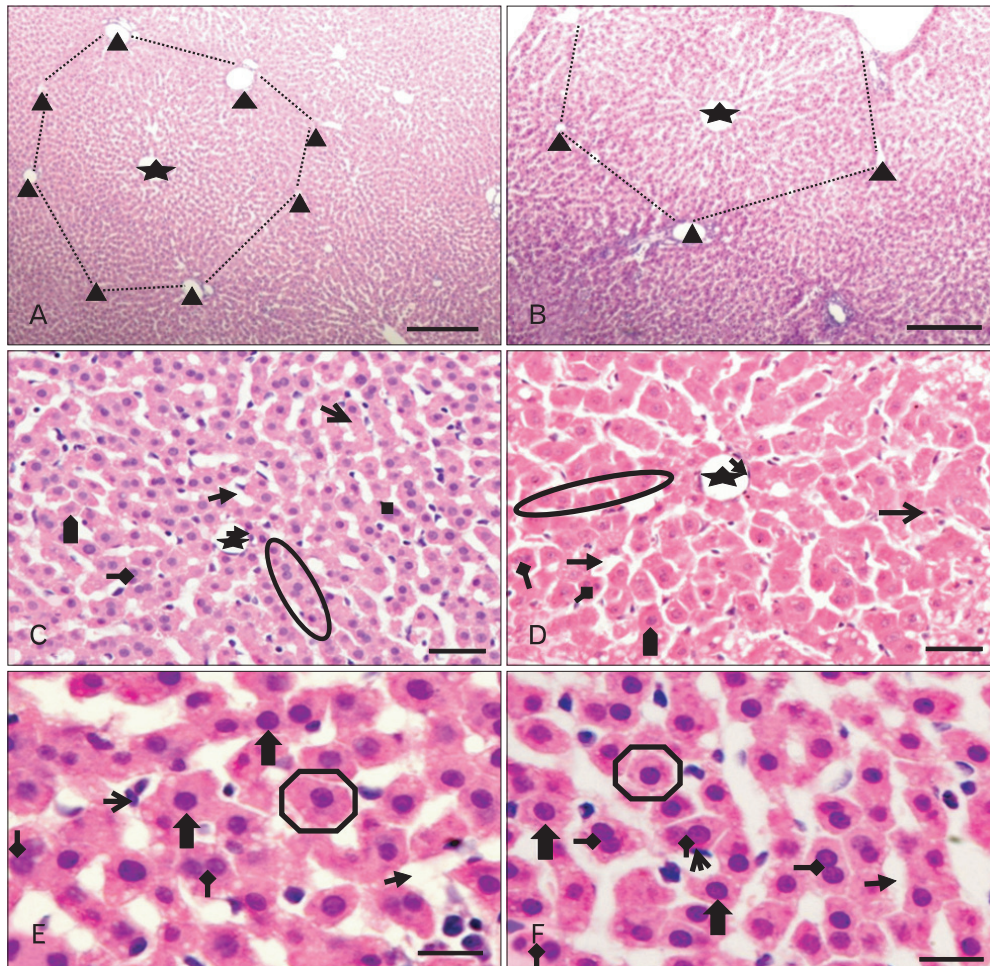
Fig. 4. Low (A, B) and high (C-F) magnification photomicrographs of hematoxylin and eosin stained sections of liver (postnatal days 29) showing: preserved classical lobular pattern (dotted outline) with the central vein (black asterisk) in the center and the portal triads (black triangles) at the corners of the lobule in (A) control and (B) experimental animals. Apparent increase in hepatocyte size (▮) and dilatation of sinusoids (➡) in experimental group (D). Single cell thick hepatocyte plates (circle), binucleate cell (➤), kupffer cell (➡), endothelial cell lining the central vein (➘) (C, D), polyhedral hepatocytes (⬡), centrally placed spherical nucleus (⬆). Scale bars=200 μm (A, B), 50 μm (C, D), 20 μm (E, F).

centrilobular areas; when compared to control group (Fig. 5A); in some of the group II sections, raising the possibility of increased fat deposition in these regions.

Morphometric observations

The hepatocytes' mean nuclear area was 28.32±0.83 μm^2 in group I and 34.42±3.28 μm^2 in group II. Their mean nuclear diameter was 5.97±0.83 μm in group I and 6.56±0.31 μm in group II. The differences were significant ($P<0.05$) (Fig. 6A, B). The percentage of uninucleate and binucleate hepatocytes was largely comparable in both groups (Fig. 6C).

SBB stained sections

The expression of SBB staining, a measure of lipid droplet

distribution, was mostly confined to the cytoplasm of the hepatocytes, with some hepatocytes showing more intense staining (Fig. 7A). The hepatic acinus, the region between a central vein and a nearby portal triad (Fig. 7A, B), was clearly demarcated, showing more intense staining in the zones closer to the central vein in both groups (Fig. 7A, B). The mean gray values for zones (1, 2, 3) between the central vein and the inter-portal triad area [19] from the six animals of each group were largely similar between group I (166.14±24, 167.95±25, and 164.35±24) and group II (166.22±17, 166.58±17, and 163.57±16) (Fig. 7C).

Glutathione (GSH) levels

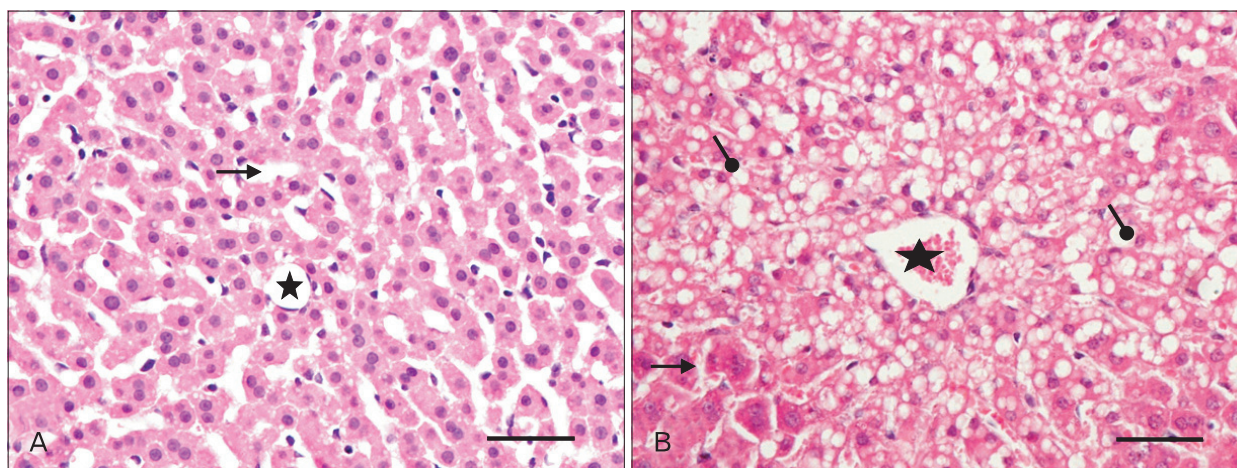The GSH level of wet liver tissue in group II (11.23±0.98

Fig. 5. High magnification photo micrographs of hematoxylin and eosin stained sections of liver (postnatal days 29) from control (A) and experimental (B) group. Intracytoplasmic vacuolization (●) around the central vein (asterisk) in (B); sinusoids (→). Sclae bars=50 μm (A, B).
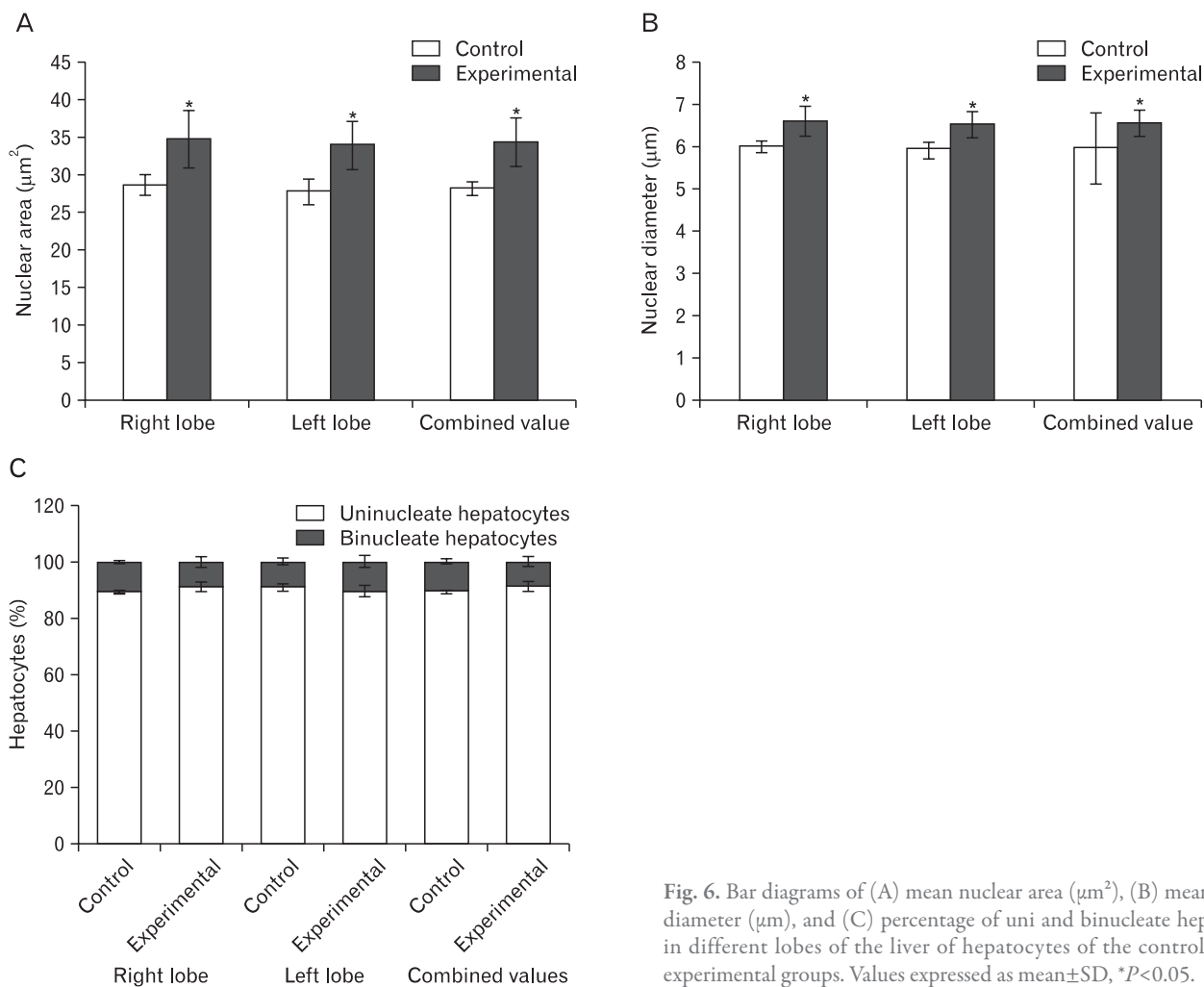

Fig. 6. Bar diagrams of (A) mean nuclear area (μm²), (B) mean nuclear diameter (μm), and (C) percentage of uni and binucleate hepatocytes in different lobes of the liver of hepatocytes of the control and the experimental groups. Values expressed as mean±SD, *$P<0.05$.
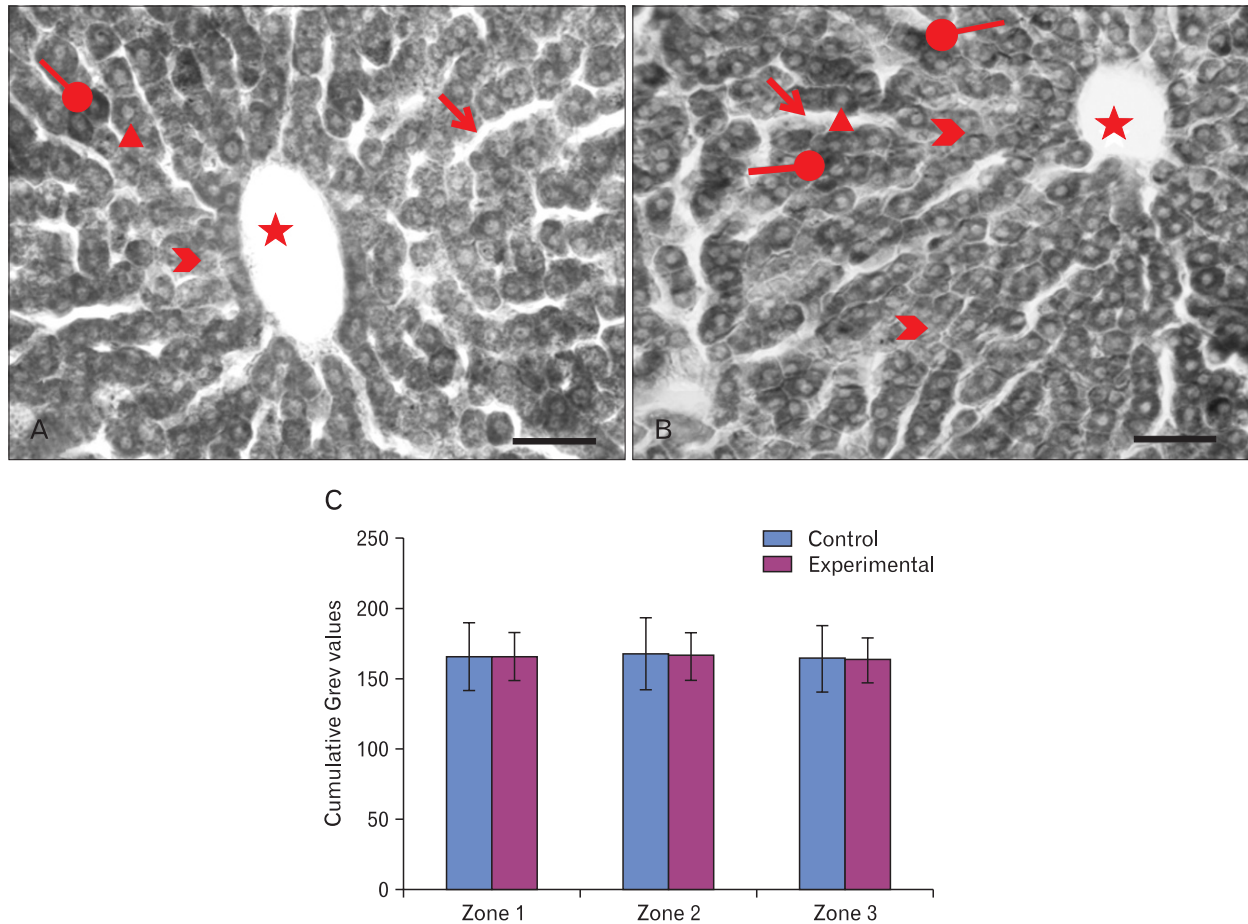
Fig. 7. High magnification photo micrographs of Sudan black B stained sections of liver (postnatal days [PND] 29) from (A) the control and (B) the experimental groups. More (—●) and less (➤) intensely stained hepatocytes, intense staining of cytoplasm against pale nuclei (triangle), central vein (asterisks); sinusoids (→). Scale bars=50 μm (A, B). (C) Bar diagram showing the mean grey values in the zones of hepatic acinus of the control and the experimental groups.

μg/g) was significantly ($P<0.05$) less than that in group I (19.72±3.63 μg/g) (Fig. 8).

Discussion

The effects of postnatal exposure (PND 9-28) to sodium arsenite on the hepatic maturation parameters of rats were assessed. The conversion of double cell plates to single cell plates [5]; increases of hepatocyte (nuclear) size [10] and the centrilobular distribution of lipid droplets [11] were measured. PND 28 in rats corresponds to five years' postnatal hepatic development in humans [5], suggesting a similar extrapolation of animal exposure effects to humans. The late fetal, the neonatal and the late suckling period have been identified as periods of enzymatic differentiation in the liver, hence the importance of cytological changes during
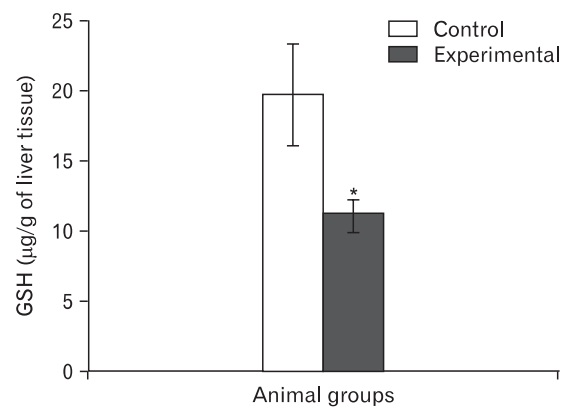

Fig. 8. Bar diagram showing the levels of reduced glutathione (GSH, μg/g of liver tissue) in the control and the experimental groups. Value expressed as mean±SD, *$P<0.05$.

these periods. Exposure to toxic stimuli during this period of functional and structural heterogeneity can adversely influence various morphological and functional parameters, thereby increasing morbidity.

The observation of no significant difference in body weight between the two groups is in accordance with earlier work [21, 22]. However, decreased body weight of rat pups has been reported subsequent to arsenic exposure (36.7 mg/l) via drinking water from PND 1 to 4 months [23]. This significant decrease likely resulted from higher dosage administer for a longer duration. In another study, no significant difference in adult rats' body weight was observed following exposure to arsenic at 5 mg/kg bw sodium arsenite [24-26]. One work has reported a dose-dependent decrease in the net gain in body weight of adult rats [27] after the inhalation exposure of arsenic trioxide (0.3, 3, and 10 mg/mg). The decrease in weight gain was associated with decreased food consumption. The present study represents a shorter duration (PND 9-28) and a low level (1.5 mg/kg body weight) of exposure to sodium arsenite, hence the observed lack of effect on body weight is not to be unexpected given previous results. As the maturational development of liver is at its peak during this period, the metabolically active cells could be presumed to be able to cope with the additional stress of the environmental insult without manifesting changes in general parameters such as body weight.

Arsenic-induced distortion of liver histology, such as sinusoidal dilatation, cellular edema, megalocytosis, vacuolation and distorted hepatocyte nuclei, have been reported [28] in Indian catfish (*Clarias batrachus* L.) following exposure to sub-lethal concentrations (0.5 μM) of arsenic. In the present study, the intervening sinusoids appeared wider in group II than in group I, consistent with the above findings. Liver sinusoidal endothelial cells possess specialized filtering functionality. They provide low-pressure, trans-endothelial transport of nutrients and wastes into and out of the liver parenchyma [29]. Progressive inflammatory angiogenesis and blood vessel remodeling of mice livers has been observed following low-level sodium arsenite exposure via drinking water [30-32]. Sinusoidal dilatation has been suggested to represent the early stages of hyperplasia of the sinusoidal lining cells [32]. These previous reports conform to the current observations of an association between exposure and consequences in endothelial cells (sinusoids) determined by dosage and duration of exposure to low levels of arsenic.

The conversion of double to single cell (hepatocyte) pla-

tes is an important parameter of hepatic maturation. The initial irregular and thick arrangement of cell plates [5] begins to straighten and thin in the centrilobular region and proceed in a centrifugal manner. Formation of two to five cell thick cords has been reported on gestational day eleven in rat embryos, with the cellular thickness decreasing with further growth [33]. The lowest and highest percentages of single cell plates in rat livers have been observed at PND 8 (16.9%) and 28 (84.6%), respectively [5]. In the present study (PND 29), almost the all plates of hepatocytes were single cell plates in both groups, suggesting that the low dose and short exposure used here may not greatly affect this ongoing maturational event. Exposure to infectious or hepatotoxic agents has been established to be related to the vulnerablity of the hyperplasia of the liver parenchyma. Two-cell thick hepatocytes plates (within the hepatic lobule) and a high nucleo-cytoplasmic ratio is a predominant feature of hepatitis B surface antigen positive adult (human) hepatocytes [34]. This suggests te integration of viral genome into the human DNA (hepatocytes) as the underlying basis for the hyperplasia (increased thickness) of hepatocyte plates [34].

Hepatocyte nuclear diameters in group I of this work were similar (4-6 μm) to those found in other works [35, 36], those in group II were significantly higher. Increased hepatocyte nuclear diameter and volume subsequent to exposure to arsenic in green sunfish has been reported [37]. Changes in hepatocyte nuclear size have also been reported following exposure to other substances. Dose-dependent initial increases from 8.24 to 8.75 μm and a later decrease to 7.34 μm following phenobarbitone exposure (5 consecutive days) has been observed [38] in a work postulating the cytoplasmic and nuclear enlargements were due to increased accumulation of phenobarbital inducing membranes in the cytoplasm and increasing mitotic activity. In other work [39, 40], phenobarbitone-induced liver growth was imputed to hepatocyte enlargement without any influence of nuclear compartment. Studies on human hepatocytes [41-45] have reported normal hepatocyte nuclears diameter of 6.5-7.3 μm, and their enlargement following hepatitis B infection.

Sodium potassium adenosine triphosphatase (Na/K ATPase) has been reported to be responsible for the energy dependent extrusion of sodium ions (Na^+) and uptake of potassium ions (K^+), an important part of the maintenance of ionic homeostasis [46]. Damage to membrane lipids with impaired Na/K ATPase functioning subsequent to arsenic induced oxidative stress could be important in altering

water/ion transport. This could lead to fluid/substances retention in cells and cell swelling. The crippling of cellular transport due to impaired ATP metabolism subsequent to arsenic or 4-hydroxy-2-nonenal (HNE; a lipid peroxidation product) exposure has been suggested [47, 48]. The competitive substitution of arsenate for inorganic phosphate [49], so that the energy generated in kreb's cycle (oxidative phosphorylation) cannot be trapped for ATP synthesis, can compromise cellular energy requirements for the ongoing synthetic processes. A time dependent reduction in hepatic plasma membrane Na/K ATPase activity has been reported in mice exposed to arsenic through drinking water [50]; an arsenic dose dependent induction of lipid peroxidation in rats has also been reported [51]. Besides arsenic, other environmental factors such as nicotine, insulin, and sodium fluoride have been implicated in affecting Na/K ATPase [52-56] and so compromising cellular energy requirements.

In the present study, group I (89.26±0.82%) and group II (90.99±1.77%) showed mainly uninucleate cells with a small remainder of binucleate cells. This is in partial agreement with another study [57], which reported 4.6% of rat hepatocytes as binuclear at day 22 and 27.5% at 25-30 days. Acytokinesis or the defective cytokinesis of mononuclear cells or the fusion of two mononuclear cells was suggested as the cause of the binucleation, which could be important cells in the genesis of tetraploid hepatocytes. Liver cell polyploidation is considered an original physiological process: cells pass through a binucleation step which enables them to increase metabolic output and constitutes an alternative to cell division. The observation of an increased number of binucleate cells following trypan blue injection in guinea pigs suggested increased mitosis as the underlying basis for increased binuclearity [58]. Rats fed high-fat diets have shown higher numerical density of binucleate hepatocytes, presumably as a compensatory response to the decreased number and size of hepatocytes following necrotic changes [59]. In the present study, the observed similarity in the percentage of uninucleate and binucleate cells between the two groups suggests that arsenic exposure at low dosage (1.5 mg/kg body weight) from PND 9-28, might not be influential in altering cells' polyploidy status.

Lipid droplet distribution shows a definitive pattern with age: there is an even distribution of lipid droplets in the centrilobular and periportal areas of newborn mice [11] and their centrilobular localization in growing animals [60, 61]. The adult pattern (more numerous in centrilobular

than in periportal hepatocytes) in mice is reached between PND 21 and 24 [11]. Therefore, lipid droplet distribution is an important parameter for evaluating the liver's lipid metabolic function, as an altered pattern suggests altered lipid function, this is in spite of lipid demonstrable in the histological sections being only a part of the hepatic lipid reserves. The observed intense fatty change in the central region of the hepatic lobule in rats after trypan blue injections suggests low oxygen tension in the central part of the lobule interfering with rapid oxidation or phosphorylation of the fat [62]. The observation of more intense staining (SBB) in zone 3 (centrilobular) than in zone 1 (periportal) was suggestive of no modification of the adult pattern of lipid droplet distribution following the exposure to arsenic-administered in this study. The formation of a fatty liver as a later development in arsenic induced toxicity, rather than reduced levels of glutathione present at an earlier period is interesting [50]. Mixed patterns of steatosis (microvesicular and macrovesicular) in the liver biopsies of hepatitis C virus patients with the fat globules initially formed in zone 3 and then coalesced to form large droplets (macrosteatosis) with associated fibrosis [20]. Microvesicular steatosis implies the presence of mitochondrial dysfunction and oxidative stress [63]. Sporadic degeneration with cytoplasmic vacuolation and necrosis in adult rat hepatocytes treated with either alcohol or arsenic points to the direct hepatotoxic effects of both; the coadministration of alcohol and arsenic also significantly increased hepatocyte degeneration and vacuolation, suggesting a synergistic hepatotoxicity [64].

The initiation of oxidative stress following exposure to hepatotoxic agents is an important factors underlying chronic liver diseases associated with fibrosis. Disturbed membrane molecular properties through damage to such as membrane lipids, building blocks of proteins (amino acids), sugars (carbohydrates) and nucleic acids, is likely the primary factor of chemical induced hepatocellular injury. The liver is the center of metabolism of various chemicals including inorganic arsenic in a number of animals including mammals [65] and reduced GSH in hepatocytes acts as a vital antioxidant. It is present at high concentrations (7-8 μM) in the liver tissue [66]. The significant decrease in GSH level in group II of the present study suggests the arsenite induced impairment of cellular antioxidant defense. Significant reduction in hepatic GSH has been reported in animals receiving sodium meta-arsenite (25 ppm) in drinking water (24 weeks) [67]. Reduced GSH in the liver tissue of rats treated with arsenic trioxide was

reversed by the administration of ascorbic acid, suggesting the role of antioxidants in ameliorating arsenic induced oxidative stress [68].

Arsenic's imbalancing of redox systems is also associated with its role as a potent inhibitor of glutathione reductase. Animals fed arsenic have been reported to show reduced levels of hepatic GSH with decreased enzymes of GSH regeneration, suggesting that arsenic induced exacerbation of toxic effects with depleted GSH levels in the liver [50]. GSH is essential for the reduction of arsenic (V) to arsenite (III) in protecting the cell against more toxic inorganic forms [69]. The biochemical observations of the present study indicate impairment of hepatocytes' GSH related antioxidant capacity due to arsenic exposure which in turn could lead to liver function derangement manifesting at a later age.

Biochemical and morphological evidence of arsenite induced hepatotoxicity was observed in developing rat livers. The evidence was reduced levels of GSH (leading to increased oxidative stress), increased size of hepatocyte nuclei, sporadic vacuolation of hepatocyes and sinusoidal dilatation in the animals administered arsenic. To understand the exact mechanisms underlying arsenic induced toxicity at cellular and molecular levels, broader studies using various dosages of sodium arsenite and varied durations of exposure at different developmental periods should be considered.

Acknowledgements

References

1. Garelick H, Jones H, Dybowska A, Valsami-Jones E. Arsenic pollution sources. Rev Environ Contam Toxicol 2008;197:17-60.
2. Hardman JG, Limbird LE, Gilman AG. Goodman & Gilman's: the pharmacological basis of therapeutics. 10th ed. New York: McGraw-Hill; 2001. p.1892-965.
3. Agency for Toxic Substances and Disease Registry. 2007. Toxicological profile for arsenic. Draft for public comment [Internet]. Atlanta: Agency for Toxic Substances and Disease Registry; 2007 [cited 2012 Nov 1]. Available from: http://www.atsdr.cdc.gov/toxprofiles/tp.asp?id=22&tid=3.
4. Sato EF, Nakagawa E, Hiramoto K, Yamamasu S, Moriyama-Shimamoto I, Inoue M. Oxidative stress promotes the regression of fetal liver hemopoiesis. Biochemistry (Mosc) 2004;69:18-22.
5. Alexander B, Guzail MA, Foster CS. Morphological changes during hepatocellular maturity in neonatal rats. Anat Rec 1997;248:104-9.
6. Liu J, Xie Y, Ward JM, Diwan BA, Waalkes MP. Toxicogenomic analysis of aberrant gene expression in liver tumors and nontumorous livers of adult mice exposed in utero to inorganic arsenic. Toxicol Sci 2004;77:249-57.
7. Ledda-Columbano GM, Coni P, Faa G, Manenti G, Columbano A. Rapid induction of apoptosis in rat liver by cycloheximide. Am J Pathol 1992;140:545-9.
8. Sell S, Salman J. Light- and electron-microscopic autoradiographic analysis of proliferating cells during the early stages of chemical hepatocarcinogenesis in the rat induced by feeding N-2-fluorenylacetamide in a choline-deficient diet. Am J Pathol 1984;114:287-300.
9. Farber E. Similarities in the sequence of early histological changes induced in the liver of the rat by ethionine, 2-acetylaminofluorene, and 3'-methyl-4-dimethylaminoazobenzene. Cancer Res 1956;16:142-8.
10. White EG. Some observations on the liver of the pig: the hepatic lobule and liver cell during post-natal growth. J Anat 1939;73(Pt 3):365-86.1.
11. Asada M, Kanamura S. Postnatal changes in the distribution of lipid droplets within the liver lobule of the mouse. J Anat 1979;129(Pt 2):423-6.
12. Moron MS, Depierre JW, Mannervik B. Levels of glutathione, glutathione reductase and glutathione S-transferase activities in rat lung and liver. Biochim Biophys Acta 1979;582:67-78.
13. Ellman GL. Tissue sulfhydryl groups. Arch Biochem Biophys 1959;82:70-7.
14. Bancroft JD, Gamble M. Theory and practice of histological techniques. 5th ed. Edinburgh: Churchill Livingstone; 2002. p.206-56.
15. Carson FL. Histotechnology: a self instructional text. Chicago: ASCP Press; 1990. p.161-2.
16. Bayliss High OB. The histochemical versatility of Sudan Black B. Acta Histochem Suppl 1981;24:247-55.
17. Shen LJ, Zhang ZJ, Ou YM, Zhang HX, Huang R, He Y, Wang MJ, Xu GS. Computed morphometric analysis and expression of alpha fetoprotein in hepatocellular carcinoma and its related lesion. World J Gastroenterol 2000;6:415-6.
18. Bjugn R. The use of the optical disector to estimate the number of neurons, glial and endothelial cells in the spinal cord of the mouse: with a comparative note on the rat spinal cord. Brain Res 1993;627:25-33.
19. Ross MH, Romrell LJ, Kaye GI. Histology: a text and atlas. 3rd ed. Philadelphia: Williams & Wilkins; 1995. p.498-500.
20. Zubair A, Jamal S, Mubarik A. Morphometric analysis of hepatic steatosis in chronic hepatitis C infection. Saudi J Gastroenterol 2009;15:11-4.
21. Dhar P, Somesh M, Kaushal P, Sehgal R, Mehra RD. Effects of arsenic exposure during early postnatal period on Leydig cells of rat testis. Toxicol Environ Chem 2010;92:1157-68.
22. Dhar P, Mohari N, Mehra RD. Preliminary morphological and morphometric study of rat cerebellum following sodium arsenite

exposure during rapid brain growth (RBG) period. Toxicology 2007;234:10-20.

23. Rodríguez VM, Carrizales L, Mendoza MS, Fajardo OR, Giordano M. Effects of sodium arsenite exposure on development and behavior in the rat. Neurotoxicol Teratol 2002;24:743-50.

24. Jana K, Jana S, Samanta PK. Effects of chronic exposure to sodium arsenite on hypothalamo-pituitary-testicular activities in adult rats: possible an estrogenic mode of action. Reprod Biol Endocrinol 2006;4:9.

25. Pant N, Murthy RC, Srivastava SP. Male reproductive toxicity of sodium arsenite in mice. Hum Exp Toxicol 2004;23:399-403.

26. Sarkar M, Chaudhuri GR, Chattopadhyay A, Biswas NM. Effect of sodium arsenite on spermatogenesis, plasma gonadotrophins and testosterone in rats. Asian J Androl 2003;5:27-31.

27. Holson JF, Stump DG, Ulrich CE, Farr CH. Absence of prenatal developmental toxicity from inhaled arsenic trioxide in rats. Toxicol Sci 1999;51:87-97.

28. Datta S, Saha DR, Ghosh D, Majumdar T, Bhattacharya S, Mazumder S. Sub-lethal concentration of arsenic interferes with the proliferation of hepatocytes and induces *in vivo* apoptosis in *Clarias batrachus* L. Comp Biochem Physiol C Toxicol Pharmacol 2007;145:339-49.

29. Braet F, Vanbesien J, De Zanger R, Wisse E. Ageing of the liver sieve and pseudocapillarisation. Lancet 2002;360:1171-2.

30. Straub AC, Stolz DB, Ross MA, Hernández-Zavala A, Soucy NV, Klei LR, Barchowsky A. Arsenic stimulates sinusoidal endothelial cell capillarization and vessel remodeling in mouse liver. Hepatology 2007;45:205-12.

31. Straub AC, Stolz DB, Vin H, Ross MA, Soucy NV, Klei LR, Barchowsky A. Low level arsenic promotes progressive inflammatory angiogenesis and liver blood vessel remodeling in mice. Toxicol Appl Pharmacol 2007;222:327-36.

32. Popper H, Thomas LB, Telles NC, Falk H, Selikoff IJ. Development of hepatic angiosarcoma in man induced by vinyl chloride, thorotrast, and arsenic. Comparison with cases of unknown etiology. Am J Pathol 1978;92:349-76.

33. Sasaki K, Matsumura G. Haemopoietic cells of yolk sac and liver in the mouse embryo: a light and electron microscopical study. J Anat 1986;148:87-97.

34. Chen ML, Gerber MA, Thung SN, Thornton JC, Chung WK. Morphometric study of hepatocytes containing hepatitis B surface antigen. Am J Pathol 1984;114:217-21.

35. McKellar M. The postnatal growth and mitotic activity of the liver of the albino rat. Am J Anat 1949;85:263-307.

36. Plenk H. Uber Anderungen der Zellgrosse im Zusammenhang mit dem Korperwachstum der Tiere. Arb Zool Inst Wien 1911;19:247-88.

37. Sorensen EM, Ramirez-Mitchell R, Pradzynski A, Bayer TL, Wenz LL. Stereological analyses of hepatocyte changes parallel arsenic accumulation in the livers of green sunfish. J Environ Pathol Toxicol Oncol 1985;6:195-210.

38. Bolender RP, Weibel ER. A morphometric study of the removal of phenobarbital-induced membranes from hepatocytes after cessation of threatment. J Cell Biol 1973;56:746-61.

39. Barka T, Popper H. Liver enlargement and drug toxicity. Medicine (Baltimore) 1967;46:103-17.

40. Kunz W, Schaude G, Schmid W, Siess M. Stimulation of liver growth by drugs. In: Proceedings of the European Society for the Study of Drug Toxicity, Vol. VII (International Congress Series No. 115); 1966 Jan; Rome. Amsterdam: Excerpta Medica Foundation; 1966. p.113-53.

41. Blendis LM, Orrego H, Crossley IR, Blake JE, Medline A, Isreal Y. The role of hepatocyte enlargement in hepatic pressure in cirrhotic and noncirrhotic alcoholic liver disease. Hepatology 1982;2:539-46.

42. Israel Y, Orrego H, Colman JC, Britton RS. Alcohol-induced hepatomegaly: pathogenesis and role in the production of portal hypertension. Fed Proc 1982;41:2472-7.

43. Watanabe T, Tanaka Y. Age-related alterations in the size of human hepatocytes. A study of mononuclear and binucleate cells. Virchows Arch B Cell Pathol Incl Mol Pathol 1982;39:9-20.

44. Orrego H, Blendis LM, Crossley IR, Medline A, Macdonald A, Ritchie S, Israel Y. Correlation of intrahepatic pressure with collagen in the Disse space and hepatomegaly in humans and in the rat. Gastroenterology 1981;80:546-56.

45. Ranek L, Keiding N, Jensen ST. A morphometric study of normal human liver cell nuclei. Acta Pathol Microbiol Scand A 1975;83:467-76.

46. Park S, Jung Y. Combined actions of Na/K-ATPase, NCX1 and glutamate dependent NMDA receptors in ischemic rat brain penumbra. Anat Cell Biol 2010;43:201-10.

47. Miyake H, Kadoya A, Ohyashiki T. Increase in molecular rigidity of the protein conformation of brain Na+-K+-ATPase by modification with 4-hydroxy-2-nonenal. Biol Pharm Bull 2003;26:1652-6.

48. Valkonen S, Savolainen H, Järvisalo J. Arsenic distribution and neurochemical effects in peroral sodium arsenite exposure of rats. Bull Environ Contam Toxicol 1983;30:303-8.

49. Forbush B 3rd. Rapid 86Rb release from an occluded state of the Na,K-pump reflects the rate of dephosphorylation or dearsenylation. J Biol Chem 1988;263:7961-9.

50. Santra A, Maiti A, Das S, Lahiri S, Charkaborty SK, Mazumder DN. Hepatic damage caused by chronic arsenic toxicity in experimental animals. J Toxicol Clin Toxicol 2000;38:395-405.

51. Ramos O, Carrizales L, Yáñez L, Mejía J, Batres L, Ortíz D, Díaz-Barriga F. Arsenic increased lipid peroxidation in rat tissues by a mechanism independent of glutathione levels. Environ Health Perspect 1995;103 Suppl 1:85-8.

52. Serhan MF, Kreydiyyeh SI. Insulin down-regulates the Na+/K+ ATPase in enterocytes but increases intestinal glucose absorption. Gen Comp Endocrinol 2010;167:228-33.

53. Rosta K, Tulassay E, Enzsoly A, Ronai K, Szantho A, Pandics T, Fekete A, Mandl P, Ver A. Insulin induced translocation of Na+/K+-ATPase is decreased in the heart of streptozotocin diabetic rats. Acta Pharmacol Sin 2009;30:1616-24.

54. Lim DK, Kim HS. Opposite modulation of glutamate uptake by nicotine in cultured astrocytes with/without cAMP treatment. Eur J Pharmacol 2003;476:179-84.

55. Suketa Y. Fundamental and applied studies on transport and metabolism of electrolytes and glucose: aim to contact with molecular biology. Yakugaku Zasshi 2002;122:507-25.

56. Harold DE, Walz W. Metabolic inhibition and electrical properties of type-1-like cortical astrocytes. Neuroscience 1992; 47:203-11.

57. Guidotti JE, Brégerie O, Robert A, Debey P, Brechot C, Desdouets C. Liver cell polyploidization: a pivotal role for binuclear hepatocytes. J Biol Chem 2003;278:19095-101.

58. Pfuhl W. Die Leber. In: Mollendorf WV, editor. Handbuch der Mikroskopischen Anatomie des Menschen. Vol. 5. Berlin: Springer; 1932. p.235-425.

59. Altunkaynak BZ, Ozbek E. Overweight and structural alterations of the liver in female rats fed a high-fat diet: a stereological and histological study. Turk J Gastroenterol 2009;20:93-103.

60. Cutts JH, Leeson CR, Krause WJ. The postnatal development of the liver in a marsupial, *Didelphis virginiana*. 1. Light microscopy. J Anat 1973;115(Pt 3):327-46.

61. Leeson CR, Cutts JH. The postnatal development of the rabbit liver. Biol Neonate 1972;20:404-13.

62. Deane HW. A cytological study of storage and secretion in the developing liver of the mouse. Anat Rec 1944;88:161-73.

63. McGovern BH, Ditelberg JS, Taylor LE, Gandhi RT, Christopoulos KA, Chapman S, Schwartzapfel B, Rindler E, Fiorino AM, Zaman MT, Sax PE, Graeme-Cook F, Hibberd PL. Hepatic steatosis is associated with fibrosis, nucleoside analogue use, and hepatitis C virus genotype 3 infection in HIV-seropositive patients. Clin Infect Dis 2006;43:365-72.

64. Flora SJ, Pant SC, Malhotra PR, Kannan GM. Biochemical and histopathological changes in arsenic-intoxicated rats coexposed to ethanol. Alcohol 1997;14:563-8.

65. Vahter M, Marafante E. Effects of low dietary intake of methionine, choline or proteins on the biotransformation of arsenite in the rabbit. Toxicol Lett 1987;37:41-6.

66. Palekar AG, Tate SS, Meister A. Decrease in glutathione levels of kidney and liver after injection of methionine sulfoximine into rats. Biochem Biophys Res Commun 1975;62:651-7.

67. Flora SJ, Chouhan S, Kannan GM, Mittal M, Swarnkar H. Combined administration of taurine and monoisoamyl DMSA protects arsenic induced oxidative injury in rats. Oxid Med Cell Longev 2008;1:39-45.

68. Saha B. Effect of ascorbic acid on reduced glutathione level in arsenic-loaded isolated liver tissues of rat. Bangladesh J Pharmacol 2006;1:68-71.

69. Vahter M. What are the chemical forms of arsenic in urine, and what can they tell us about exposure? Clin Chem 1994;40:679-80.